Electronic Supplementary Information

Mechanoresponsive and Recyclable Biocatalytic Sponges from Enzyme-Polymer Surfactant Conjugates and Nanoparticles

Table of Contents:

1. Experimental:

(i) Fabrication of biocatalytic sponges for GOx-PS/HRP-PS based cascade reaction:

To a 10 % (w/v) solution of silica nanoparticles, 10 mg of 25 kDa PEI (from 100 mg mL^{-1} stock solution) was added and vortexed for 10 minutes to form a layer-by-layer assembly of the PEI on the nanoparticles surface. To the resultant colloidal solution, 0.5 mL of GOx-PS (0.2 mg mL^{-1}) solution and HRP-PS (0.2 mg mL^{-1}) solution was added and stirred for 10 min. Further, 5 mg of PEGDE (from 100 mg ml^{-1} stock solution) was used to cross-link the protein clusters with PEI coated silica nanoparticles and frozen for 24 hours at -20°C, similar to the procedure in the literature.[1] After 24 hours, the sponge was thawed and washed with ample amount of MilliQ water to ensure removal of excess unreacted PEGDE.

(ii) Calculations related to Compression studies:

Calculation for product (pNP) formation:

The enzymatic conversion of para-nitrophenyl phosphate (pNPP) into para-nitrophenolate ion (pNP) by alkaline phosphatase (ALP; which mediates cleavage of phosphate bond under alkaline conditions) was monitored using UV-Vis spectrophotometer. The amount of product formed was measured at 410 nm (λ_{max} of pNP). Absorbance values were obtained directly from the spectrophotometer as raw inputs for calculating ALP activity in the form of nALP/cALP/ALP-PS conjugate clusters. In the current system, the nALP/ALP-PS were immobilized inside Silica-PEI/Silk-PEI based sponges which serve as reaction centers. The concentration of product pNP obtained could be determined by absorbance values of pNP which diffused back in the aqueous solution after the reaction. However, since the sponges harbor positively charged PEI polymer chains, some amount of product, pNP (negatively charged), formed during enzymatic hydrolysis of substrate gets adhered to the sponges. Therefore, in order to determine the enzyme activity, product formation should be measured accurately and this necessitated removal of pNP which was electrostatically adhered to the sponges. Hence, the sponges were washed with 100 mM NaCl aqueous solution, to screen the interactions between pNP and PEI, and finally remove the entire trapped product. After this, the recorded absorbance (A) was divided by the extinction coefficient (ϵ) of pNP (i.e. 18.6 $mM^{-1}cm^{-1}$), the obtained value was multiplied by a factor of 1000 for mM to μM conversion. This was further multiplied by volume (Dilution factor; D) of NaCl required for washing which provided with a total concentration of pNP formed in micromoles. (*Eq. 1*)

- *Concentration of pNP = (Absorbance × 1000 × Dilution Factor)/ Molar Extinction Coefficient*

$$[\text{pNP}] = (A \times 1000 \times D) / \epsilon \quad \text{.....(Eq. 1)}$$

(iii) Calculations related to Kinetic (Michaelis Menten) studies:

To determine the hydrolytic capacity of immobilized nALP/ALP-PS (within the sponges), small cylindrical sponges (total sponge volume = 0.7 mL; containing 0.25 mg total protein) were used. These sponges were equilibrated to ambient temperature prior to assay. For these experiments at 37 ° C, the sponge was suspended in the reaction cuvette with the help of a non-interacting thread, and the substrate solution was stirred continuously at 200 rpm by using rice size magnetic needle to ensure complete mixing of all components and to avoid diffusion limitations. Kinetic mode in the UV-Vis spectrophotometer was used to measure the absorbance at 410 nm continuously for 15 minutes. At a particular substrate concentration, observed absorbance value was divided by the extinction coefficient (18.6 mM^{-1} cm^{-1}) and multiplied by the unit conversion factor of 1000 (for converting millimoles to micromoles). Further, product formed (μM) was plotted against time of incubation to obtain a straight line where the product formation was linearly proportional with respect to time, indicating initial velocity (represented by slope of straight line) at that substrate concentration in terms of μM/min (termed as velocity V_1).

However, some of the product was entrapped inside sponge due to electrostatic interactions between the negatively charged pNP and positively charged PEI. In order to determine complete product formation (indicating rate of reaction) 100 mM NaCl aqueous solution was used for washing the sponges and release pNP in solution for measuring absorbance. The reattainement in colour of the sponges from bright yellow to snow white was used as an indication for the removal of all the adhered pNP to the sponges. The wash volume was finally collected and absorbance was determined at 410 nm using spectrophotometer; this value corresponded to the amount of product formed at the end of incubation (i.e. 15 minutes). The velocity of formation of this product was assumed to be linear, and therefore total amount of product formed (calculated from the absorbance value as per *Eq. 1*) was divided by incubation time to obtain velocity of reaction in terms of μM min^{-1} (termed as velocity V_2).

Absolute initial velocity of reaction was obtained by addition of V_1 and V_2 at a particular substrate concentration; similar calculations were performed for each substrate concentration. Further, graph of substrate concentration *vs* initial velocities was plotted which provided with

a hyperbolic relationship. This complete data represented a change in initial velocity of enzyme reaction with respect to substrate concentration. Michalies-Menten fitting (using Origin software fnction) was used to calculate various parameters for enzyme kinetics *viz.* V_{max} (maximum initial velocity- correlated as enzyme activtiy), K_M (Michaelis-Menten constant- signifies the affinity of enzyme towards given substrate), k_{cat} (turnover number- indicating number of substrate molecules converted in per unit time) and k_{cat}/K_M (catalytic efficiency- accounts for substrate binding and conversion to product). V_{max} and K_M were computed from Michaelis Menten fitting or Lineweaver-Burk plot; k_{cat} was calculated by dividing V_{max} with enzyme concentration (in μM). These all parameters were useful for comparison of variants of same enzyme in terms of their catalytic activity.

$$V_1 = \frac{\partial\,[pNP]}{\partial t} \quad \text{……(Eq. 2)}$$

V_1 = Initial velocity as obtained from absorbance values from continuous assay of sponge at 410 nm for 15 minutes.

[*p*NP] = Concentration of pNP formed calculated from absorbance obtained from continuous assay in μM.

$$V_2 = \frac{(A \times 1000 \times D)/\epsilon}{t} \quad \text{…….(Eq. 3)}$$

V_2 = Initial velocity as obtained from absorbance values from washing out the entrapped product [pNP] in the sponge after 15 minutes.

t = total incubation time for which the product was trapped inside sponge i.e, 15 minutes.

Initial Velocity; $V = V_1 + V_2$

(xi) Characterization techniques

(a) Matrix Assisted Laser Desorption/Ionization-Time of Flight (MALDI-TOF):

Matrix Assisted Laser Desorption/Ionization-Time of Flight spectra were collected on a Bruker Autoflex Speed instrument to determine the cationization efficiency of ALP. The samples were incorporated in a sinapinic acid matrix, dissolved in 0.1% Acetonitrile and 0.1% TFA. The net volume ratio of protein samples to matrix was kept at 1:1. Studies showed an increase in mass of 4000 g mol^{-1} for native ALP (nALP) 37000 g mol^{-1} to 41000 g mol^{-1} (Figure

S2) after cationization with DMAPA (mol. wt. = 102 g mol^{-1}) in the presence of EDC indicating 73% cationization efficiency.

(b) Dynamic Light Scattering (DLS) & Zeta potential:

Dynamic Light Scattering and Zeta potential studies were performed on Anton Par Litesizer™ 500 for determining the size and charge of nALP, cALP, ALP-PS, Silica NPs-PEI and Silica NPs-PEI / ALP-PS clusters, RSF and Silk nanoparticles. The percentage number average and Potential were measured for dilute samples prepared in water, filtered using 0.22 µm syringe filter at room temperature (Figure S1).

(c) Circular Dichroism (CD):

Circular Dichroism measurements were performed using a Spectropolarimeter (JASCO J-815, Tokyo, Japan) to determine the secondary structures of nALP, cALP, ALP-PS. The measurements were conducted using a quartz cuvette of 1cm path length, in a wavelength range of 180-260nm with data integration time of 2 seconds and data interval of 20 nm. The final concentration of all protein samples was maintained in the range of 0.1 - 0.01 mg ml^{-1} and was measured before-hand with the help of UV-Vis spectrophotometer. The raw CD data was normalized and background corrected. The relative percentage of secondary structure was obtained using the web-based server DichroWeb using CDSSTR algorithm. Fitted data was plotted with the experimental data between 240 to 190 nm (Figure 1d).

(d) UV-Visible spectroscopy based activity profiles for control studies:

Control studies were performed on ALP-PS less Silica NPs-PEI sponge, nALP sponge, cALP sponge and ALP-PS sponge. All the sponges were equilibrated at room temperature after the addition of 1.5 mL pNPP solution (5 mM pNPP in 100 mM glycine Buffer with 1mM $MgCl_2$, pH 8.8) for ten minutes after which the product was compressed out and complete absorbance spectra was measured in UV-Vis Spectrophotometer without any dilution. pNPP showed an absorption maxima at 305 nm while, the product pNP absorbed at 410 nm (Figure S5).

2. Figures:

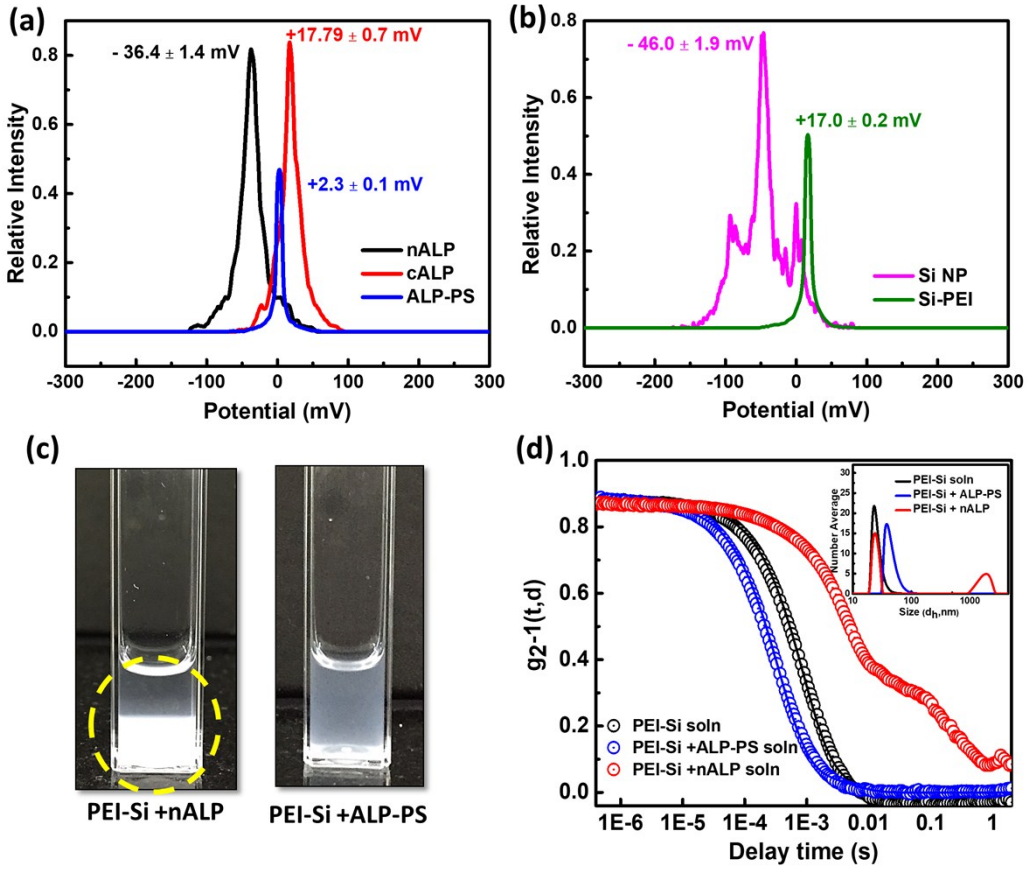

Figure S1: (a) Zeta potential charge distribution on native ALP (n ALP) -36.4 ± 1.4 mV at physiological pH, cationized ALP (cALP) after diamine coupling of acidic residues in nALP +17.79 ± 0.7 mV, polymer surfactant bioonjugated ALP (ALP-PS) after surface neutralization of cALP with negatively charged polymer surfactant S_1 +2.3 ±0.1 mV. (b) Zeta potential charge distribution for Pristine silica nanoparticles -46.0 ±1.9 mV and PEI coated Silica NPs +17.0 ± 0.2 mV (c) Optical images showing the two final solutions used for sponge formation (left) PEI-SI + nALP undergoes phase seperation after just 20 min. due to formation of complex aggregates as evident from DLS data (d) showing presence of particles having 1500 nm hydrodynamic radis in the solution, while (right) PEI-SI + ALP-PS solution remains homogenously dispersed even after keeping for 24 hours, with DLS data showing no signs of aggregation. (d) Dynamic Light Scattering (DLS) plot of decay for autocorrelation function (g_2-1(t,d)) with respect to delay time (s) and inset showing number average distribution for (a) PEI-SI Soln 46 ± 6 nm, PEI-SI + ALP-PS Soln 38 ± 4 nm and PEI-SI + nALP 50 ± 5 nm and 1500 ± 50 nm.

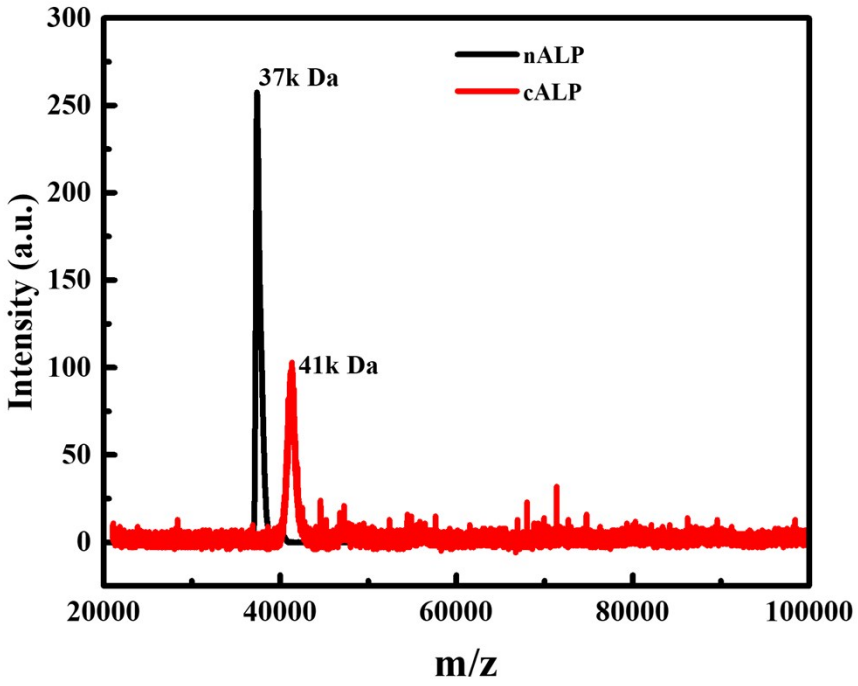

Figure S2: MALDI-TOF spectra showing peaks for native ALP (nALP) at 37 kDa and cationized ALP (cALP) at 41 kDa with a mass increment of 4kDa, leading to cationization efficiency of ~ 73% out of total 53 acidic amino groups (Glutamic and Aspartic acid residues) present in nALP . After cationization total number of positively charged groups after EDC coupling (38 DMAPA coupled acidic groups + 41 basic groups (Lysines +Arginines) present on cALP are 79.

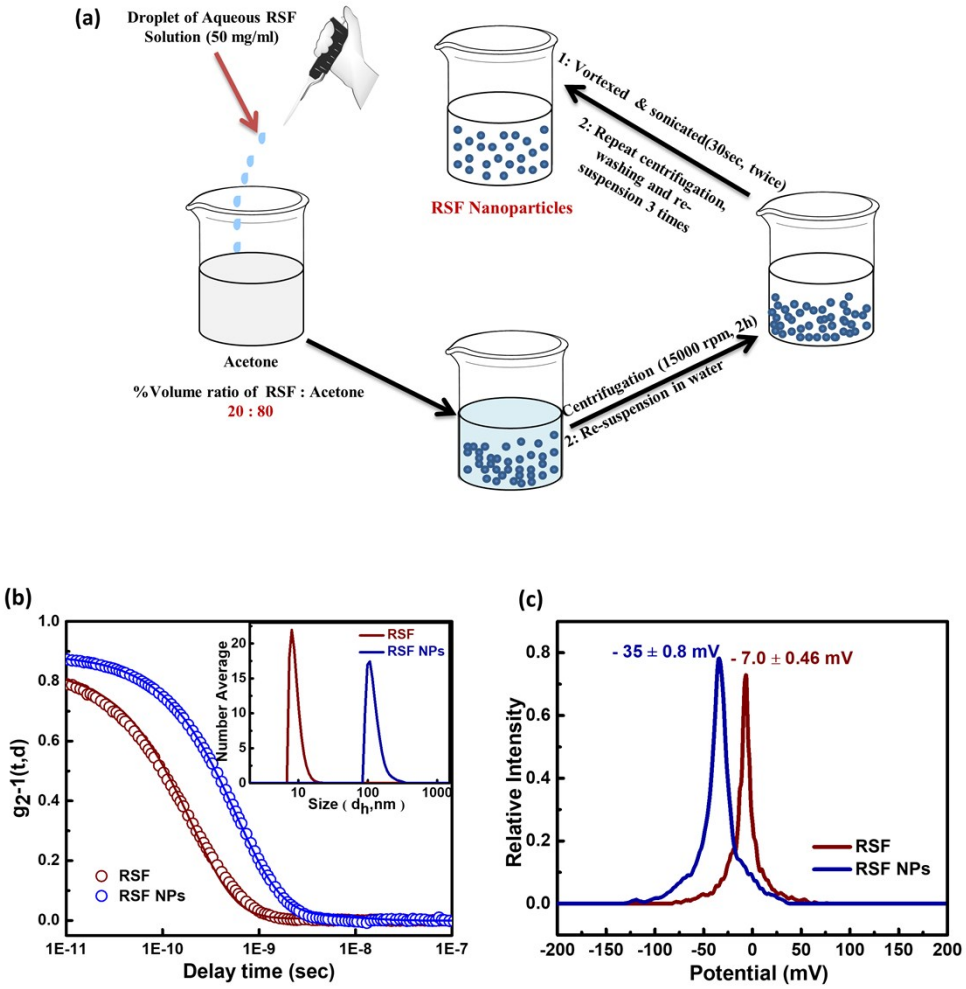

Figure S3: (a) Schematic showing synthesis of Silk nanoparticles from Regenerated Silk Fibroin using *desolvation* method**.** Silk Nanoparticles precipitate down after dropwise addition of RSF (50 mg ml^{-1}) into acetone in 20:80 ratio of RSF: Acetone to maintain > 80% v/v acetone volume. The Nanoparticles formed are centrifuged out at 15000 rpm for 2hours and re-dispersed in water and repeat sonicated to remove aggregates, if any. (b) Dynamic Light Scattering (DLS) plot of decay for autocorrelation function ($g_{2\text{-}1}(t,d)$) with respect to delay time (s) Silk Fibroin (RSF) 8.02 ± 0.4 nm and Regenerated Silk nanoparticles (Silk NPs) 106 ± 10 nm. (c) Zeta potential charge distribution Regenerated Silk fibroin (RSF) -35.0 ± 0.8 mV and PEI coated Silk NPs -7.0 ± 0.46 mV.

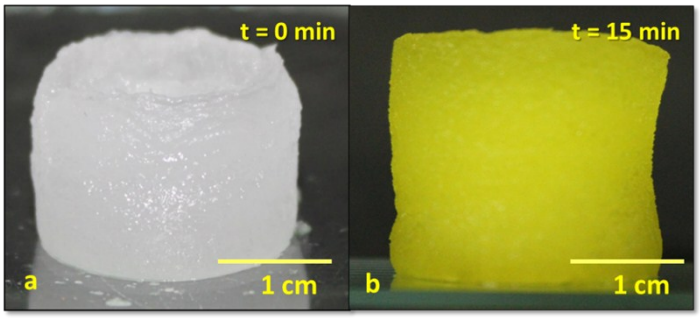

Figure S4: Optical Image showing PEI coated silk nanoparticle (Silk-NPs-PEI) and ALP-PS based biodegradable biocatalytic sponge. (a) Before addition of pNPP substrate, the sponge has been equilibrated at room temperature. (b) After 15 minutes of addition of 1.5 ml pNPP substrate (15.2 mM) in 100 mM glycine buffer and 1 mM $MgCl_2.6H_2O$ at pH 8.8 kept at room temperature. The product formed can be extruded out and observed at 410 nm for pNP using UV-Vis spectrophotometer.

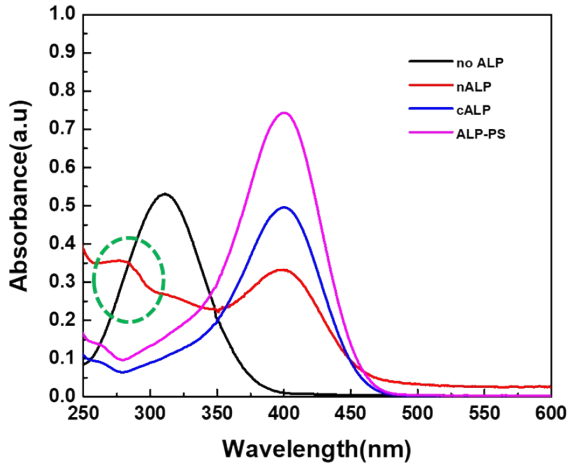

Figure S5: UV-Visible spectroscopy based activity profiles for control studies: The above graph shows pNP formation in different Silica NPs-PEI sponges containing no ALP, native ALP, cALP and ALP-PS. All the sponges were equilibrated at room temperature after the addition of pNPP 5 mM in 100 mM glycine buffer with 1mM $MgCl_2$, pH 8.8 for ten minutes after which the product pNP was compressed out. The absorbance at 305 nm in no ALP sponge shows presence of pNPP indicating no reaction taking place in the sponge. Two peaks at 410 nm and 280 nm are observed in the case of sponge containing nALP where the former is indicative of formation of pNP in the sponge while the later represents leeching of nALP in the system. In case of cALP and ALP-PS conjugate sponges only one peak for formation of pNP was observed at 410 nm.

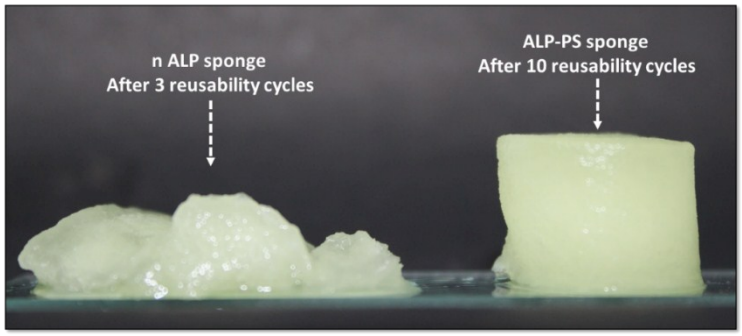

Figure S6: Optical Image of nALP/ ALP-PS and Silica NPs-PEI sponge after different reusability cycles. The nALP sponge breaks after undergoing only 3 reusability cycles while ALP-PS sponge even after 10 reusability cycle (with each reusability cycle having 10 C-D repetitions with 1 C-D min^{-1}; total 100 C-D cycles) maintains its structural robustness and elasticity.

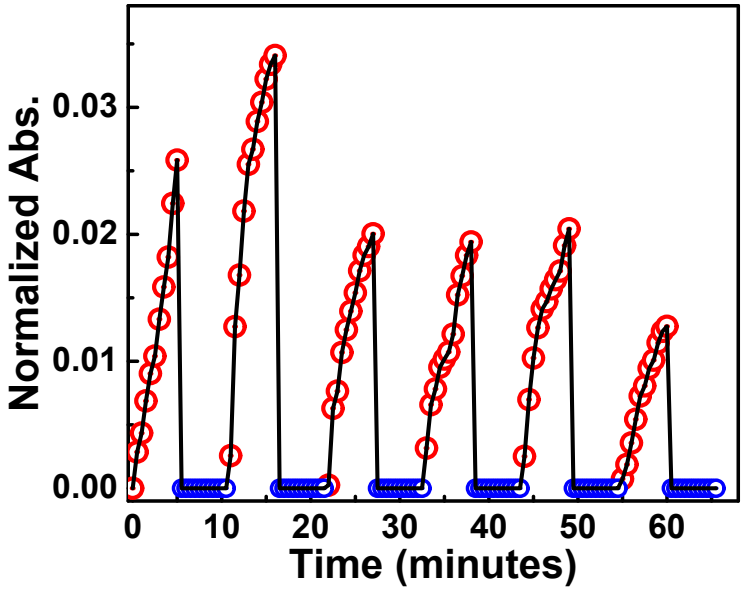

Figure S7: Time dependent UV-Vis spectra showing the normalized absorbance for the ON-OFF switch of ALP-PS based Silica-PEI NPs sponge cycled 6 times in the presence of pNPP solution, with complete set (ON; red circles and OFF; blue circles) lasting for 10 minutes at 37 $^{\circ}$C. ON set showed an increase in the concentration of pNP which was monitored at 410 nm, while OFF set showed no formation of pNP. During the ON state of the switch (and from the 2nd set onwards), at least two different rates of reactions can be visualized as indicated by different slopes of absorbance *vs* time. This suggests that the absorbed pNPP within the biocatalytic sponge continues to undergo pNP conversion in the OFF state.

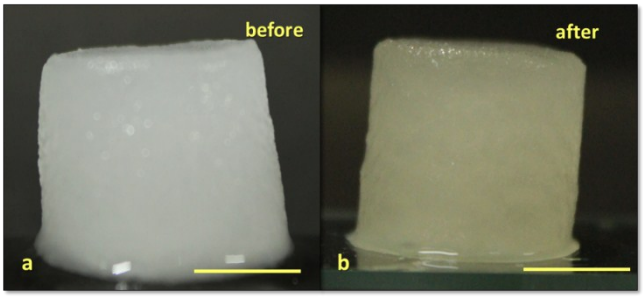

Figure S8: Optical Images showing dual enzyme based biocatalytic Silica-PEI NPs sponges for GOx-PS + HRP-PS cascade conversion of D-glucose. (a) A white sponge of silica NPs-PEI/GOx-PS+HRP-PS before its insertion into a 250 mL beaker containing substrate solution comprising 15 mL D-glucose (100 mM) and ABTS 5 mL (3mM) in sodium phosphate buffer at pH 7. (b) The biocatalytic sponge after removing from the substrate solution. Almost entire colored product (oxidised ABTS) formed by the biocatalytic reaction occurring inside the sponge could be extruded out by simple compression of the sponges and subsequently, a minimal washing was required. This could be understood as a result of repulsion between similarly charged oxidised $ABTS^{+\bullet}$ and PEI polymer due to which the product dispersed in the solution immediately when sponge was immersed in the bulk substrate solution.

3. Tables:

Table 1: Percentage Secondary Structure as obtained from fitting CD data using CDSSTR algorithm as presented in Figure 1d.

Sample	α-helix	β-strand	β-turns	Unordered
nALP	0.18	0.32	0.20	0.30
cALP	0.16	0.28	0.20	0.36
ALP-PS	0.07	0.32	0.22	0.39

Table 2: Concentration of pNP formed in consecutive ten reusability cycles performed on the same sponge as presented in Figure 5c in the main manuscript.

No. of reusability cycles	1	2	3	4	5	6	7	8	9	10
Conc. of pNP formed (μM)	18.18	17.92	16.04	15.96	14.62	14.37	12.61	11.12	10.59	10.42

Table 3: Concentration of pNP formed in biocatalytic sponge with C-D cycles varying from 0 to 4 min^{-1} for different time intervals. As depicted in Figure 5d the concentration of product formed increases with increase in C-D frequency.

Time (min.)	0 C-D min^{-1} [pNP] (μM)	1 C-D min^{-1} [pNP] (μM)	2 C-D min^{-1} [pNP] (μM)	4 C-D min^{-1} [pNP] (μM)
0	0	0	0	0
5	4.46 ± 0.9	7.4 ± 0.7	10.05 ± 1.5	12.1 ± 1.4
10	8.92 ± 1.2	18.84 ± 3.3	24.77 ± 1.6	39.1 ± 3.2
15	13.35 ± 3.9	50.20 ± 4.8	64.37 ± 5.3	103.25 ± 4.1
20	15.42 ± 3.6	84.9 ± 7.2	118.94 ± 9.6	154.22 ± 8.5
25	24.52 ± 4.4	126.5 ± 15.0	155.48 ± 10.5	190.1 ± 9.2